

TabKAN: Advancing Tabular Data Analysis using Kolmogorov-Arnold Network

Ali Eslamian¹, Alireza Afzal Aghaei², Qiang Cheng^{1,3*}

¹Department of Computer Science, University of Kentucky, 329 Rose Street, Lexington, 40506, Kentucky, USA.

²Independent Researcher.

³Institute for Biomedical Informatics, University of Kentucky, 800 Rose Street, Lexington, 40506, Kentucky, USA.

Abstract

Tabular data analysis presents unique challenges due to its heterogeneous feature types, missing values, and complex interactions. While traditional machine learning methods, such as gradient boosting, often outperform deep learning approaches, recent advancements in neural architectures offer promising alternatives. This paper introduces TabKAN, a novel framework that advances tabular data modeling using Kolmogorov-Arnold Networks (KANs). Unlike conventional deep learning models, KANs leverage learnable activation functions on edges, which improve both interpretability and training efficiency. Our contributions include: (1) the introduction of modular KAN-based architectures for tabular data analysis, (2) the development of a transfer learning framework for KAN models that supports knowledge transfer between domains, (3) the development of model-specific interpretability for tabular data learning, which reduces dependence on post hoc and model-agnostic analysis, and (4) comprehensive evaluation of vanilla supervised learning across binary and multi-class classification tasks. Through extensive benchmarking on diverse public datasets, TabKAN demonstrates superior performance in supervised learning while significantly outperforming classical and Transformer-based models in transfer learning scenarios. Our findings highlight the advantage of KAN-based architectures in transferring knowledge across domains and narrowing the gap between traditional machine learning and deep learning for structured data.

1 Introduction

Tabular data is a fundamental form of structured data commonly observed across diverse domains, including healthcare, finance, e-commerce, and scientific research. Analyzing such data efficiently and accurately is critical for deriving actionable insights and improving decision-making processes. Despite significant progress in deep learning, particularly in image and text processing, tabular data analysis remains a challenging area due to its unique characteristics, such as heterogeneous feature types, missing values, and complex feature interactions. While traditional machine learning methods, such as tree-based models, have often shown stronger performance than deep learning approaches in this domain, the development of novel architectures specific to tabular data remains important.

In recent years, the potential of neural networks for tabular data modeling has gained increasing attention. Among these, Kolmogorov-Arnold Networks (KANs) have emerged as a promising alternative to traditional Multi-Layer

Perceptrons (MLPs), addressing key challenges such as interpretability, training efficiency, and robustness. Unlike MLPs, which rely on fixed activation functions at nodes, KANs use learnable activation functions on edges that permits more flexible and efficient modeling of complex feature interactions. Inspired by the Kolmogorov-Arnold representation theorem, which expresses any multivariate continuous function as a composition of univariate functions and a summation operator, KANs offer a structured framework for tabular data analysis.

This paper introduces TabKAN, a framework for numerical and categorical feature encoding through a KAN-based module developed specifically for tabular data modeling using various KAN-based architectures, including spline-KAN [1], ChebyshevKAN [2], RKAN [3], Fourier KAN [4], fKAN [5], and Fast-KAN [6]. Due to the diversity and complexity of patterns in tabular datasets, TabKAN uses multiple KAN variants to allow flexible adaptation and improved representation capacity suited to different data characteristics. The primary novelties of this study are:

- The introduction of modular KAN-based architectures for tabular data analysis
- The development of a transfer learning framework for KAN models that supports knowledge transfer between domains
- The creation of model-specific interpretability methods for tabular data learning that reduce reliance on post hoc analysis
- A comprehensive evaluation of vanilla supervised learning across binary and multi-class classification tasks

TabKAN demonstrates stable and significantly improved performance in supervised learning and transfer learning tasks, outperforming baseline models in binary and multi-class classification across diverse public datasets. By applying KAN principles, TabKAN unifies traditional machine learning and deep learning, providing a robust, interpretable, and efficient solution for tabular data modeling.

Unlike traditional regression-based approaches used to explore factors affecting health-related quality of life [7], TabKAN offers a novel, attention-based method suitable for modeling complex interactions in healthcare data.

2 Related Work

Existing methods for tabular learning face multiple obstacles, such as mismatched feature sets between training and testing, limited or missing labels, and the potential emergence of new features over time [8]. These methods can be categorized as:

Classic Machine Learning Models. Early techniques rely on parametric or non-parametric strategies like K-Nearest Neighbors (KNN), Gradient Boosting, Decision Trees, and Logistic Regression [9]. Popular models include Logistic Regression (LR), XGBoost [10, 11], and MLP. A notable extension is the self-normalizing neural network (SNN) [12], which uses scaled exponential linear units (SELU) to maintain neuron activations at zero mean and unit variance. While SNNs are simple and effective, they can fail on complex, high-dimensional data, which has led to the proposal of more advanced neural architectures.

Deep Learning-Based Supervised Models. Building on Transformer architectures, methods such as AutoInt [13] apply self-attention to learn feature importance, while TransTab [14] extends Transformers to handle partially overlapping columns across multiple tables. This extension supports tasks such as transfer learning, incremental feature learning, and zero-shot inference. TabTransformer [15] applies self-attention to improve feature embeddings and achieves strong performance even with missing data. SAINT [16] introduces hybrid attention at both row and column levels, pairs it with inter-sample attention and contrastive pre-training, and outperforms gradient boosting models including XGBoost [10], CatBoost [17], and LightGBM [18] on several benchmarks.

Other innovations include TabRet [19], which implements a retokenization step for previously unseen columns, and XTab [20], which enables cross-table pretraining in a federated learning setup, handling heterogeneous column types and numbers. TabCBM [21] introduces concept-based explanations that support human oversight, balancing predictive accuracy and interpretability. TabPFN [22] is a pretrained Transformer that performs zero-shot classification on tabular data through meta-learning, without requiring task-specific training. TabMap [23] transforms tabular data into 2D topographic maps that encode feature relationships spatially and preserve values as pixel intensities. This structure allows convolutional networks to detect association patterns efficiently and outperforms other deep learning-based supervised models. TabSAL [24] employs lightweight language models to generate privacy-free synthetic tabular data

when raw data cannot be shared due to privacy concerns. TabMixer [25] builds on the MLP-mixer framework and captures both sample-wise and feature-wise interactions through a self-attention mechanism.

3 Background

3.1 Data Preprocessing

To address missing values and class imbalance, we adopted the preprocessing strategy introduced in [25]. Let the input variable space be defined as $\mathcal{Data} \in \{\mathbb{R} \cup \mathbb{C} \cup \mathbb{B} \cup \emptyset\}$, where \mathbb{R} , \mathbb{C} , and \mathbb{B} denote the domains of numerical, categorical, and binary data, respectively. After the preprocessing block, we denote the resulting feature-target pair as $\{\mathcal{X}, \mathcal{Y}\}$, where x contains numerical features, and y is an integer used in classification tasks. The label set $\{\mathcal{Y}\}$ may have dimension one for binary classification or M for multi-class classification.

Most tabular datasets contain both continuous numerical and categorical variables. We preprocess the categorical features by converting them into one-hot vectors. After preprocessing, the data is organized as an $n \times m$ matrix with purely numerical entries.

3.2 Kolmogorov-Arnold Networks (KANs)

3.2.1 Spline Kolmogorov-Arnold Network

A general KAN network is a composition of L layers. Given $\mathbf{x}_0 \in \mathbb{R}^{n_0}$, the output is

$$\text{KAN}(\mathbf{x}_0) = (\Phi_{L-1} \circ \dots \circ \Phi_0) \mathbf{x}_0.$$

For scalar outputs (i.e., $n_L = 1$), we denote

$$f(\mathbf{x}) = \text{KAN}(\mathbf{x}),$$

and it can be expanded analogously using a nested summation form. The original Kolmogorov-Arnold representation [26] corresponds to a 2-layer KAN of shape $[n, 2n + 1, 1]$; nonlinearities sit on the edges, while each node simply sums its inputs. A natural way to approach the underlying approximation problem is by selecting appropriate univariate functions $\phi_{q,p}$ and Φ_q . In this setup, the middle layer has width $2n + 1$. However, a two-layer spline-based network often lacks sufficient expressivity for complex tasks. Consequently, we generalize the KAN design by making it both deeper and wider.

This construction mirrors that of MLPs, where a single layer, an affine transformation followed by a nonlinearity, is stacked to increase model capacity. Similarly, we define a KAN layer and compose multiple such layers to build a deeper, more expressive model.

Let the network’s shape be an integer array

$$[n_0, n_1, \dots, n_L],$$

where n_ℓ denotes the number of nodes in the ℓ -th layer. Denote the activation of the i -th neuron in the ℓ -th layer by $x_{\ell,i}$. Between layer ℓ and layer $\ell + 1$, there are $n_\ell \times n_{\ell+1}$ univariate functions $\phi_{\ell,j,i}$. For the connection from neuron (ℓ, i) to $(\ell + 1, j)$, the input is $x_{\ell,i}$ and the output (post-activation) is

$$\tilde{x}_{\ell,j,i} = \phi_{\ell,j,i}(x_{\ell,i}).$$

Each neuron $(\ell + 1, j)$ sums all post-activations from its incoming edges:

$$x_{\ell+1,j} = \sum_{i=1}^{n_\ell} \phi_{\ell,j,i}(x_{\ell,i}).$$

In matrix form, layer ℓ can be expressed as

$$\mathbf{x}_{\ell+1} = \begin{pmatrix} \phi_{\ell,1,1}(\cdot) & \cdots & \phi_{\ell,1,n_\ell}(\cdot) \\ \vdots & \ddots & \vdots \\ \phi_{\ell,n_{\ell+1},1}(\cdot) & \cdots & \phi_{\ell,n_{\ell+1},n_\ell}(\cdot) \end{pmatrix} \mathbf{x}_\ell,$$

where Φ_ℓ is the “function matrix” for the ℓ -th KAN layer. Stacking these KAN layers yields a deep KAN with greater flexibility and expressive power than the simple two-layer variant.

To define a spline KAN layer with n_{in} -dimensional inputs and n_{out} -dimensional outputs, consider a matrix of one-dimensional functions:

$$\Phi = \{\phi_{q,p}\}, \quad p = 1, \dots, n_{\text{in}}, \quad q = 1, \dots, n_{\text{out}}$$

where each $\phi_{q,p}$ has trainable parameters. In the original Kolmogorov-Arnold theorem, the “inner” functions form a KAN layer with $n_{\text{in}} = n$ and $n_{\text{out}} = 2n + 1$, while the “outer” functions form another KAN layer with $n_{\text{in}} = 2n + 1$ and $n_{\text{out}} = 1$. Since these operations are all differentiable, we train KANs through standard backpropagation.

3.2.2 Chebyshev Kolmogorov-Arnold Network Layer (ChebyKAN)

The ChebyKAN [2] employs Chebyshev polynomials of the first kind, $\{T_k(x)\}_{k=0}^d$, to approximate nonlinear functions with fewer parameters than traditional MLPs. First, the input $\mathbf{x} \in \mathbb{R}^n$ is normalized to $[-1, 1]$ via the hyperbolic tangent function:

$$\tilde{\mathbf{x}} = \tanh(\mathbf{x}).$$

The Chebyshev polynomials are then computed up to degree d using the recursive definition

$$\begin{aligned} T_0(x) &= 1, \\ T_1(x) &= x, \\ T_k(x) &= 2xT_{k-1}(x) - T_{k-2}(x), \quad \text{for } k \geq 2, \end{aligned}$$

yielding a polynomial tensor \mathbf{T} .

Let $\Theta \in \mathbb{R}^{n \times m \times (d+1)}$ be the trainable coefficient tensor for n input features, m outputs, and polynomial degree $d + 1$. The output of the ChebyKAN layer is computed via Einstein summation:

$$y_{bo} = \sum_{i=1}^n \sum_{k=0}^d T_{bik} \Theta_{io k}, \quad (1)$$

where b indexes the batch. By optimizing Θ during training, ChebyKAN learns a highly expressive mapping with exceptional accuracy, capitalizing on the orthogonality and rapid convergence of Chebyshev polynomials.

3.2.3 Fast Kolmogorov-Arnold Network (Fast KAN)

FastKAN [6] is a reengineered variant of KAN designed to significantly enhance computational efficiency by replacing the original 3rd-order B-spline basis with Gaussian radial basis functions (RBFs). In this framework, Gaussian RBFs serve as the primary nonlinear transformation, effectively approximating the B-spline operations used in traditional KAN. In addition, it applies layer normalization [27] to keep inputs from drifting outside the effective range of these RBFs. Together, these adjustments simplify the overall design of FastKAN while preserving its accuracy. The output of an RBF network is a weighted linear combination of these radial basis functions. Mathematically, an RBF network with N centers can be expressed as:

$$f(x) = \sum_{i=1}^N w_i \phi(\|\mathbf{x} - \mathbf{c}_i\|),$$

where w_i are the learnable parameters or coefficients, and ϕ is the radial basis function, which depends on the distance between the input x and a center c_i represented as:

$$\phi(r) = \exp\left(-\frac{r^2}{2h^2}\right),$$

While standard KAN consists of sums of univariate transformations to approximate multivariate functions, Fast KAN generalizes this principle in a deeper feedforward architecture. For an input vector $\mathbf{x} \in \mathbb{R}^d$, the output is computed as

$$\mathbf{y} = f_L \circ f_{L-1} \circ \dots \circ f_1(\mathbf{x}).$$

3.2.4 Padé Rational Kolmogorov-Arnold Network (PadéRKAN)

The Padé Rational Kolmogorov-Arnold Network (PadéRKAN) [3] augments the Kolmogorov-Arnold framework by adopting the Padé approximation, which expresses a function as the ratio of two polynomials:

$$R(x) = \frac{P_q(x)}{Q_k(x)} = \frac{\sum_{i=0}^q a_i x^i}{\sum_{j=0}^k b_j x^j}.$$

In each PadéRKAN layer, this rational form acts as the activation function. This structure allows the model to capture asymptotic behavior and abrupt transitions with greater precision. Specifically, for an input $\mathbf{x} \in \mathbb{R}^d$, the layer outputs

$$\mathbf{y} = \frac{\sum_{i=0}^q \theta_i P_i(\mathbf{x})}{\sum_{j=0}^k \theta_j Q_j(\mathbf{x})},$$

where θ_i and θ_j are learnable parameters for the numerator and denominator polynomials, respectively.

3.2.5 Fourier Kolmogorov-Arnold Network (Fourier KAN)

Fourier KAN [28] uses a Fourier series expansion to capture both low- and high-frequency components in tabular or structured data. Given an input vector $\mathbf{x} \in \mathbb{R}^d$, the transformation function $\phi_F(\mathbf{x})$ introduces sine and cosine terms up to a grid size g , which allows the network to approximate highly complex or oscillatory functions. Formally,

$$\phi_F(\mathbf{x}) = \sum_{i=1}^d \sum_{k=1}^g (a_{ik} \cos(k x_i) + b_{ik} \sin(k x_i)),$$

where a_{ik} and b_{ik} are trainable coefficients. The hyperparameter g controls the number of frequency components and balances representational power against computational cost.

A Fourier KAN layer applies this frequency-based feature mapping to each input dimension and then combines the resulting terms via learnable parameters. For example, an output neuron y is computed as:

$$y = \sum_{i=1}^d \sum_{k=1}^g \left(W_{ik}^{(c)} \cos(k x_i) + W_{ik}^{(s)} \sin(k x_i) \right) + b, \quad (2)$$

where $W_{ik}^{(c)}$ and $W_{ik}^{(s)}$ are learnable weights for the cosine and sine terms, respectively, and b is a bias. By using the orthogonality of trigonometric functions, Fourier KAN often achieves faster convergence than traditional MLPs and polynomial-based KANs while also reducing overfitting.

3.2.6 Fractional Kolmogorov-Arnold Network (fKAN)

The Fractional Kolmogorov-Arnold Network (fKAN) [29] incorporates fractional-order Jacobi functions into the Kolmogorov-Arnold framework to enhance expressiveness and adaptability. Each layer of fKAN uses a Fractional Jacobi Neural Block (fJNB), which introduces a trainable fractional parameter ν to adjust the polynomial basis dynamically. For an input $\mathbf{x} \in \mathbb{R}^d$, the fractional Jacobi polynomial $J_n^{(\alpha, \beta, \nu)}(x)$ is given by:

$$J_n^{(\alpha, \beta)}(x^\nu) = \frac{(\alpha + 1)_n}{n!} \sum_{k=0}^n \binom{n}{k} \frac{(\beta + 1)_{n-k}}{(\alpha + \beta + 1)_{n-k}} \left(\frac{x^\nu - 1}{2} \right)^k \left(\frac{x^\nu + 1}{2} \right)^{n-k},$$

where $(\alpha, \beta) > -1$ determine the shape of the polynomial. Within fKAN, each layer applies a linear transformation followed by a fractional Jacobi activation. This structure allows the model to capture subtle data patterns.

3.2.7 Rational Kolmogorov-Arnold Network (RKAN)

The Jacobi Rational Kolmogorov-Arnold Network (RKAN) [30] integrates Jacobi polynomials $J_n^{(\alpha, \beta)}(x)$ and a rational mapping $\phi(x, L) = \frac{x}{\sqrt{x^2 + L^2}}$ to enhance nonlinear function approximation beyond the conventional $[-1, 1]$ domain. For an input $\mathbf{x} \in \mathbb{R}^d$, the layer output is formulated as:

$$\mathbf{y} = \sum_{n=0}^N \theta_n J_n^{(\alpha, \beta)}(\phi(\mathbf{x}, L)),$$

where θ_n and L are trainable coefficients and $\alpha, \beta > -1$ specify the polynomial's orthogonality weight function $\omega(x) = (1 - x)^\alpha (1 + x)^\beta$. The mapping $\phi(x, L)$ extends the polynomials to the infinite interval, making it needless for data scaling.

3.3 Neural Architecture Search

Neural Architecture Search (NAS) is the automated process of identifying optimal neural network configurations for a specific learning task. It replaces manual architecture design with a systematic exploration of hyperparameters to improve model performance. In our study, we employ the Optuna framework [31], which efficiently navigates the search space through Bayesian optimization and pruning strategies. For each KAN variant, we perform a dedicated NAS procedure to determine the most effective combination of architecture and functional parameters.

For FastKAN, we tune the number of layers L , the width vector $\mathbf{w} = (w_1, \dots, w_L)$, and the parameters of the RBF activation functions. In PadéRKAN, we optimize network depth, layer widths, and the polynomial degrees (q, k) . For FourierKAN, the grid size g , which controls the frequency resolution of the Fourier expansion, is selected through NAS. The fKAN model includes hyperparameters such as depth, widths, and the Jacobi polynomial order. Finally, RKAN uses NAS to select depth, widths, and Jacobi polynomial order to adapt the rational architecture to varying dataset complexities.

All models are trained using the L-BFGS optimizer with cross-entropy loss. Validation F1 score is used as the selection criterion, ensuring that the chosen configurations generalize well while adapting to specific structural and statistical properties of the data. The results and analysis of these hyperparameter optimization procedures are reported in Appendix A.

4 Experiments and Results

We evaluate our model on ten publicly available datasets across both supervised and transfer learning tasks. While multiple performance metrics are computed—AUC, F1 score, precision, and recall—we report only AUC due to its effectiveness in summarizing classification performance and limitations on space. To assess robustness, we compare our model with state-of-the-art baselines under varying data and feature configurations. Following the protocol in [14],

we use average ranking as the main comparison criterion, which provides an overall view of relative performance across datasets.

4.1 Datasets

We employ a variety of datasets to evaluate our models, covering a broad spectrum of application areas:

- **Financial Decision-Making:** Credit-g (CG) and Credit-Approval (CA) datasets
- **Retail:** Dresses-sale (DS) dataset, capturing detailed sales transactions
- **Demographic Analysis:** Adult (AD) and 1995-income (IO) datasets, containing income and census-related variables
- **Specialized Industries:**
 - Cylinder bands (CB) dataset for manufacturing
 - Blastchar (BL) dataset for materials science
 - Insurance company (IC) dataset offering insights into the insurance domain

Table 1: Dataset details including abbreviation, number of classes, number of data points, and number of features.

Dataset Name	Abbreviation	# Class	# Data	# Features
Credit-g	CG	2	1,000	20
Credit-Approval	CA	2	690	15
Dataset-Sales	DS	2	500	12
Adult	AD	2	48,842	14
Cylinder-Bands	CB	2	540	35
Blastchar	BL	2	7,043	35
Insurance-Co	IO	2	5,822	85
1995-Income	IC	2	32,561	14
ImageSegmentation	SG	7	2,310	20
ForestCovertime	FO	7	581,012	55

We choose the configuration that yields the highest validation performance and then train the model on each dataset using ten distinct random seeds to mitigate the impact of training variability. This procedure aligns with the comparative approach used in TabMixer [25]. All experiments run on an AMD Ryzen Threadripper PRO 5965WX 24-core CPU with 62 GB of RAM and an NVIDIA RTX A4500 GPU featuring 20 GB of memory. To improve inference efficiency while preserving accuracy, we used PyTorch’s `torch.quantization` package to implement both static and dynamic post-training quantization, as well as quantization-aware training (QAT) [32]. This reduced the memory footprint of some models by 3% to 15%, without a significant loss in accuracy.

4.2 Baseline Models for Comparison

We benchmark our proposed model against both classic and cutting-edge techniques, including **Logistic Regression (LR)**, **XGBoost** [10], **MLP**, **SNN** [12], **TabNet** [33], **DCN** [34], **AutoInt** [13], **TabTransformer** [15], **FT-Transformer** [35], **VIME** [36], **SCARF** [37], **CatBoost** [17], **SAINT** [16], and **TransTab** [14]. These baselines span a range of approaches for tabular data, from traditional machine learning to the latest deep learning methods.

To ensure a fair comparison, we apply the same preprocessing and evaluation workflow across all models. After preprocessing, each dataset is divided into training, validation, and test sets with a 70/10/20 split.

4.3 Supervised Learning

Table 2 presents results from evaluating classical baselines (LR, XGBoost, MLP, SNN), specialized tabular models (TabNet, DCN, AutoInt, TabTrans, FT-Trans, VIME, SCARF, TransTab), and a range of KAN variants (ChebyshevKAN, JacobiKAN, PadeRKAN, Fourier KAN, fKAN, fast-KAN) alongside the original KAN architecture. Each approach is optimized individually, with hyperparameters tuned to account for differences in model structure and dataset characteristics. The results shows Chebyshev KAN emerges as the top performer, suggesting that its Chebyshev polynomial basis effectively captures intricate decision boundaries while maintaining stability. However, certain KAN variants, such as wav-KAN [38], did not show strong performance on any dataset, while others, like fc-KAN [39], feature a heavier architecture that limits practical applicability. This highlights the inherent difficulty of designing a single architecture that performs uniformly well across diverse data distributions, leading us to exclude them from our final results.

The KAN-based methods consistently outperform conventional baselines and, in many cases, are comparable to or surpass transformer-based architectures. This highlights the expressive power of the Kolmogorov-Arnold framework. Our experiments underscore the importance of careful model selection and tuning of architectural and layer-specific parameters. Moreover, the broad success of KAN variants demonstrates how leveraging polynomial, rational, or Fourier expansions can significantly improve learning on tabular data.

Table 2: Evaluation of Different Models for Supervised Learning

Methods	CG	CA	DS	AD	CB	BL	IO	IC	Rank (Std) ↓	Average ↑
Logistic Regression	0.720	0.836	0.557	0.851	0.748	0.801	0.769	0.860	17 (2.45)	0.768
XGBoost	0.726	0.895	0.587	0.912	0.892	0.821	0.758	0.925	9.06 (6.67)	0.814
MLP	0.643	0.832	0.568	0.904	0.613	0.832	0.779	0.893	15.3 (3.13)	0.758
SNN	0.641	0.880	0.540	0.902	0.621	0.834	0.794	0.892	13.6 (4.73)	0.763
TabNet	0.585	0.800	0.478	0.904	0.680	0.819	0.742	0.896	17.1 (3.49)	0.738
DCN	0.739	0.870	0.674	<u>0.913</u>	0.848	0.840	0.768	0.915	7.69 (4.12)	0.821
AutoInt	0.744	0.866	0.672	<u>0.913</u>	0.808	<u>0.844</u>	0.762	0.916	7.94 (4.63)	0.816
TabTrans	0.718	0.860	0.648	0.914	0.855	0.820	0.794	0.882	11.1 (5.85)	0.811
FT-Trans	0.739	0.859	0.657	<u>0.913</u>	<u>0.862</u>	0.841	0.793	0.915	8.19 (4.46)	0.822
VIME	0.735	0.852	0.485	0.912	0.769	0.837	0.786	0.908	11.8 (4.58)	0.786
SCARF	0.733	0.861	0.663	0.911	0.719	0.833	0.758	0.919	11 (4.56)	0.800
TransTab	0.768	0.881	0.643	0.907	0.851	0.845	0.822	0.919	<u>6.88 (3.43)</u>	0.830
TabMixer	0.660	0.907	0.659	0.900	0.829	0.821	0.974	0.969	7.94 (6.54)	0.840
KAN	0.806	0.870	0.616	0.907	0.739	0.844	0.956	0.902	8.69 (4.11)	0.83
ChebyshevKAN	0.823	0.883	0.670	0.905	<u>0.862</u>	0.859	0.951	0.905	5.88 (3.47)	0.857
JacobiRKAN	0.854	0.860	0.685	0.888	0.611	0.814	<u>0.957</u>	0.885	11.5 (7.69)	0.819
PadeRKAN	0.826	0.855	0.670	0.868	0.778	0.808	0.952	0.856	12.4 (6.52)	0.827
Fourier KAN	0.771	0.870	0.650	0.906	0.820	0.649	0.879	<u>0.935</u>	9.31 (5.08)	0.810
fKAN	<u>0.848</u>	0.870	0.691	0.892	0.692	0.811	0.954	0.890	10.2 (6.64)	0.831
fast-KAN	0.854	<u>0.897</u>	<u>0.688</u>	0.892	0.767	0.837	0.960	0.887	7.44 (6.55)	<u>0.848</u>

Supervised learning requires ample labeled data; however, recent studies improve analysis using hybrid domain-specific methods [40], multimodal approaches that combine language models with tabular inputs [41], or integrations of vision and tabular data for medical prediction tasks [42].

4.4 Transfer Learning

Transfer learning permits machine learning models to leverage knowledge acquired from a source task to enhance performance on a related target task through fine-tuning. Although this paradigm has proven effective in domains

such as computer vision and natural language processing, where shared structures simplify knowledge transfer, its application to tabular data presents unique challenges. Feature heterogeneity, dataset-specific distributions, and the absence of universal structural patterns often lead to encoder overspecialization in conventional supervised pretraining. In this scenario, models trained with a classification objective develop representations that become overly specific to dominant patterns in the source data, which restricts their adaptability to target tasks with divergent feature spaces, class imbalances, or differing objectives.

To systematically evaluate transfer learning in tabular settings, we adopt the methodology of [14] and partition each dataset into two subsets, Set1 and Set2, with a controlled 50% feature overlap. This design introduces a domain shift by treating overlapping features as shared knowledge while regarding non-overlapping features as distinct statistical domains. The partial overlap allows an assessment of the model’s ability to generalize shared representations while adjusting to novel features.

The process involves two primary stages: pretraining and fine-tuning. During pretraining, the model receives supervised training on Set1 to acquire initial feature representations. Once convergence is achieved, all layers except for the final main layer (and the bias layer, if applicable) are frozen, thereby preserving the learned patterns. Subsequently, the model undergoes fine-tuning on Set2, with only the unfrozen layers being updated. This selective updating permits the model to adapt to the target data distribution of Set2 while retaining the knowledge acquired from Set1.

Robustness is validated by evaluating the model on the test split of Set2 to measure its capacity to generalize under domain shifts. In addition, we reverse the roles of Set1 and Set2 in a cross-validation framework, which ensures a comprehensive assessment of bidirectional knowledge transfer. This approach allows TabKAN to balance stability in feature representations with adaptability through targeted fine-tuning, thereby addressing the challenges posed by feature heterogeneity and encoder overspecialization in tabular data.

As shown in Table 3, Fourier KAN attains the highest average performance among all KAN-based architectures (0.859) and ranks second overall across all evaluated models, outperforming both Transformer-based and classical approaches. Its Fourier series expansion proves particularly effective for transfer learning. The smooth, periodic basis functions approximate both low- and high-frequency components, which supports adaptation to varying feature distributions across source and target domains.

Other KAN variants such as JacobiKAN (0.814), ChebyshevKAN (0.796), and the base KAN model (0.774) also achieve strong results, often outperforming standard baselines such as XGBoost (0.776), MLP (0.775), and Transformer-based methods including TabTransformer (0.764), AutoInt (0.754), and DCN (0.758).

Table 3: Evaluation of Models for Transfer Learning

Methods	CG		CA		DS		AD		CB		BL		IO		IC		Rank(Std) ↓	Average ↑
	set1	set2	set1	set2	set1	set2	set1	set2	set1	set2	set1	set2	set1	set2	set1	set2		
Logistic Regression	0.69	0.69	0.81	0.82	0.47	0.56	0.81	0.81	0.68	0.78	0.77	0.82	0.71	0.81	0.81	0.84	14.5 (2.82)	0.736
XGBoost	0.72	0.71	0.85	0.87	0.46	0.63	0.88	<u>0.89</u>	<u>0.80</u>	0.81	0.76	0.82	0.65	0.74	0.92	<u>0.91</u>	9.53 (5.38)	0.776
MLP	0.67	0.70	0.82	0.86	0.53	<u>0.67</u>	<u>0.89</u>	0.90	<u>0.73</u>	<u>0.82</u>	0.79	0.83	0.70	0.78	0.90	0.90	9.84 (4.23)	0.775
SNN	0.66	0.63	0.85	0.83	0.54	0.42	0.87	0.88	0.57	0.54	0.77	0.82	0.69	0.78	0.87	0.88	14.5 (3.90)	0.727
TabNet	0.60	0.47	0.66	0.68	0.54	0.53	0.87	0.88	0.58	0.62	0.75	0.83	0.62	0.71	0.88	0.89	15.9 (4.09)	0.692
DCN	0.69	0.70	0.83	0.85	0.51	0.58	0.88	0.74	0.79	0.78	0.79	0.76	0.70	0.71	0.91	0.90	11.4 (4.51)	0.758
AutoInt	0.70	0.70	0.82	0.86	0.49	0.55	0.88	0.74	0.77	0.79	0.79	0.76	0.71	0.72	0.91	0.90	11.6 (4.39)	0.754
TabTrans	0.72	0.72	0.84	0.86	0.54	0.57	0.88	0.90	0.73	0.79	0.78	0.81	0.67	0.71	0.88	0.88	11.5 (3.57)	0.764
FT-Trans	0.72	0.71	0.83	0.85	0.53	0.64	<u>0.89</u>	0.90	0.76	0.79	0.78	0.84	0.68	0.78	0.91	<u>0.91</u>	8.84 (3.82)	0.781
VIME	0.59	0.70	0.79	0.76	0.45	0.53	0.88	0.90	0.65	0.81	0.58	0.83	0.67	0.70	0.90	0.90	14.5 (5.37)	0.718
SCARF	0.69	0.72	0.82	0.85	0.55	0.64	0.88	<u>0.89</u>	0.77	0.73	0.78	0.83	0.71	0.75	0.90	0.89	10.1 (2.87)	0.778
TransTab	0.74	0.76	0.87	0.89	0.55	0.66	0.88	0.90	0.80	0.80	0.79	0.84	0.73	0.82	0.91	<u>0.91</u>	5.56 (2.17)	0.803
TabMixer	0.86	<u>0.84</u>	<u>0.87</u>	<u>0.88</u>	0.64	0.71	0.90	0.90	0.94	0.77	0.93	0.92	0.95	0.95	<u>0.94</u>	0.95	1.91 (1.14)	0.883
KAN	0.80	0.81	0.86	0.86	0.50	0.50	0.56	0.64	0.73	0.74	0.84	0.85	0.95	0.95	0.90	0.90	9.19 (6.18)	0.774
ChebyshevKAN	0.79	0.76	0.89	0.89	0.60	0.60	0.84	0.88	0.77	0.50	0.65	<u>0.86</u>	<u>0.91</u>	<u>0.89</u>	0.82	0.82	8.38 (5.71)	0.796
JacobiKAN	<u>0.85</u>	0.86	0.85	0.86	<u>0.66</u>	<u>0.68</u>	0.86	0.88	0.61	0.61	0.82	0.82	0.95	0.95	0.88	0.88	8.28 (5.88)	0.814
PadeKAN	0.76	0.77	0.87	0.80	0.50	0.62	0.86	0.50	0.64	0.64	0.66	0.66	0.88	0.76	0.63	0.50	13.7 (5.51)	0.691
Fourier KAN	0.83	0.82	0.89	0.88	0.67	<u>0.68</u>	0.90	0.90	0.86	0.86	0.85	0.85	0.95	0.95	0.95	0.90	2.72 (1.56)	0.859
fKAN	0.76	0.74	0.82	0.78	0.57	0.58	0.68	0.78	0.60	0.63	0.64	0.68	0.80	0.77	0.74	0.72	14.2 (4.77)	0.704
Fast-KAN	0.71	0.81	0.84	0.75	0.57	0.53	0.66	0.71	0.63	0.62	0.73	0.70	<u>0.89</u>	0.85	0.70	0.70	13.8 (5.53)	0.713

4.5 Multi-class Classification

Table 4 presents a comparison between TabKAN and several neural network baselines on two multi-class classification benchmarks. Since these tasks often involve class imbalance, macro-F1 was selected as the primary evaluation metric during training to ensure balanced performance across all classes [43]. All KAN variants consistently outperform baseline models, with JacobiKAN achieving the highest overall performance. Its use of Jacobi polynomials, parameterized by α and β , provides a more adaptable polynomial basis, which supports improved approximation of complex patterns.

TabTrans does not have the capability to handle categorical input, so we could not run the SA dataset on it [43].

Table 4: Comparison of different methods on SG and FO datasets.

Methods	SA		FO		Rank ↓
	ACC	F1	ACC	F1	
MLP	90.97	90.73	67.09	48.03	9.25 (0.5)
TabTrans	-	-	68.76	49.47	8.5 (0.707)
TabNet	96.09	94.96	65.09	52.52	7.25 (2.5)
KAN	96.32	96.33	85.11	84.80	4 (1.15)
ChebyshevKAN	96.54	96.54	82.67	82.38	4 (3.46)
JacobiKAN	<u>96.49</u>	<u>96.49</u>	96.56	96.56	1.5 (0.577)
PadeRKAN	94.81	94.78	92.95	92.94	5.5 (2.89)
Fourier KAN	95.89	95.89	84.55	84.42	5.62 (0.479)
fKAN	95.89	95.93	<u>95.80</u>	<u>95.79</u>	<u>3.38 (1.70)</u>
fast-KAN	95.45	95.44	87.13	86.98	5.25 (1.5)

4.6 Interpretability

For interpretability purposes, there are two main approaches: model-specific methods and model-agnostic methods. Model-specific methods apply only to a particular model (e.g., in LR, coefficients represent feature importance). In contrast, model-agnostic methods can be applied to any model, regardless of its type.

A defining strength of KAN lies in their inherent interpretability, a critical advantage for domains requiring transparency in decision-making. Unlike traditional black-box models (e.g., deep neural networks or gradient-boosted trees), KANs explicitly parameterize univariate functions along network edges, enabling direct visualization of feature-wise contributions and functional mappings. This architectural design not only reduces reliance on post hoc interpretation methods but also aligns model behavior with domain-specific knowledge, fostering trust and facilitating model audits.

Figures 1, 2, and 3 illustrate the attribution of Feature 1 in the CA dataset towards the output, while Figures 4, 5, and 6 represent the attribution of Feature 2. Specifically, Figures 1 and 4 demonstrate the interpretability of the Fourier-based KAN, whereas Figures 2 and 5 highlight the interpretability of the Chebyshev-based KAN. The domain and co-domain are normalized for these figures, which explains the difference in scale compared to the Partial Dependence Plot (PDP) figures. We employed PDP as a post-hoc analysis to assess the differences in feature interpretation.

In our framework, each feature’s learned univariate function provides non-parametric insights into its contribution to the final prediction. Visualization of these functions reveals how individual features transform inputs in nonlinear ways, uncovering monotonic trends, thresholds, or saturation effects that may align with known domain behavior.

The model’s structure also supports investigation of feature interactions. Although KANs model univariate functions explicitly, deeper layers combine these mappings additively, allowing complex multivariate dependencies to emerge. Co-variations across learned functions of related features can indicate latent interactions, which are then compared with domain knowledge. For instance, overlapping saturation patterns in multiple feature mappings may reflect synergistic influence.

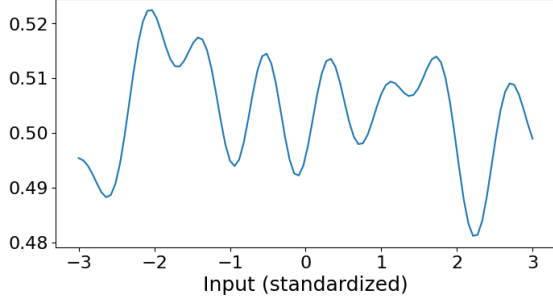


Fig. 1: Attribution of Feature 1 toward the output prediction using the Fourier KAN

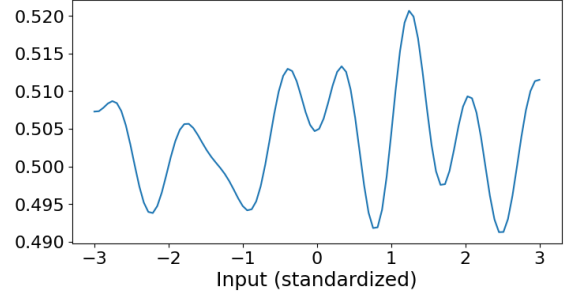


Fig. 4: Attribution of Feature 2 toward the output prediction using the Fourier KAN

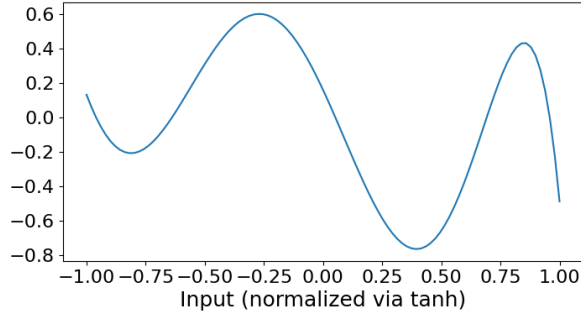


Fig. 2: Attribution of Feature 1 toward the output prediction using the ChebyshevKAN

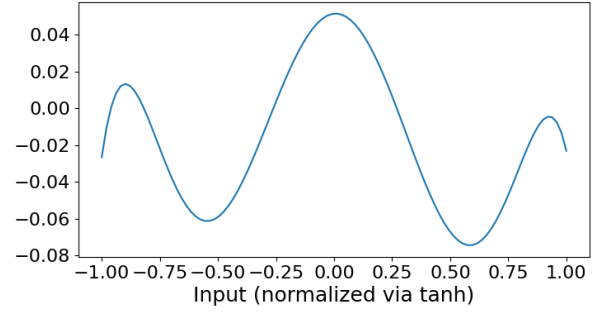


Fig. 5: Attribution of Feature 2 toward the output prediction using the ChebyshevKAN

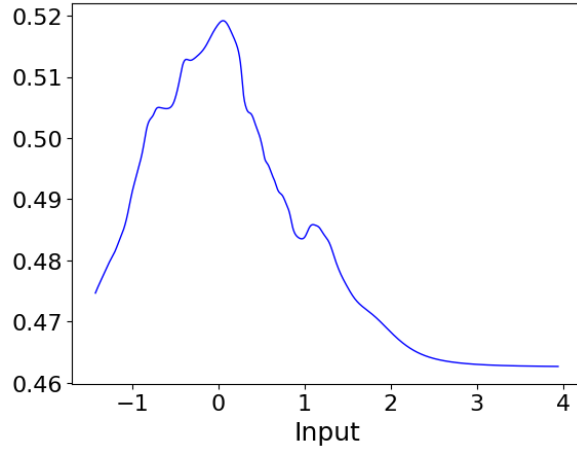


Fig. 3: Partial Dependence Plot - Feature 1

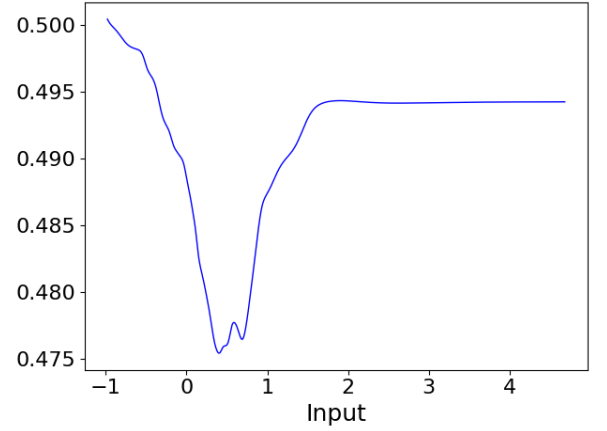


Fig. 6: Partial Dependence Plot - Feature 2

Finally, the parametric nature of KANs ensures reproducibility in interpretation. Unlike post hoc methods (e.g., SHAP or LIME), which can vary with input perturbations, KANs provide consistent functional mappings tied directly to the model's architecture.

4.7 Feature Importance and Dimensionality Reduction

We evaluate the feature importance and dimensionality reduction capabilities of the proposed TabKAN framework by analyzing the magnitude of coefficients derived from the Chebyshev and Fourier-based KAN equations. Specifically,

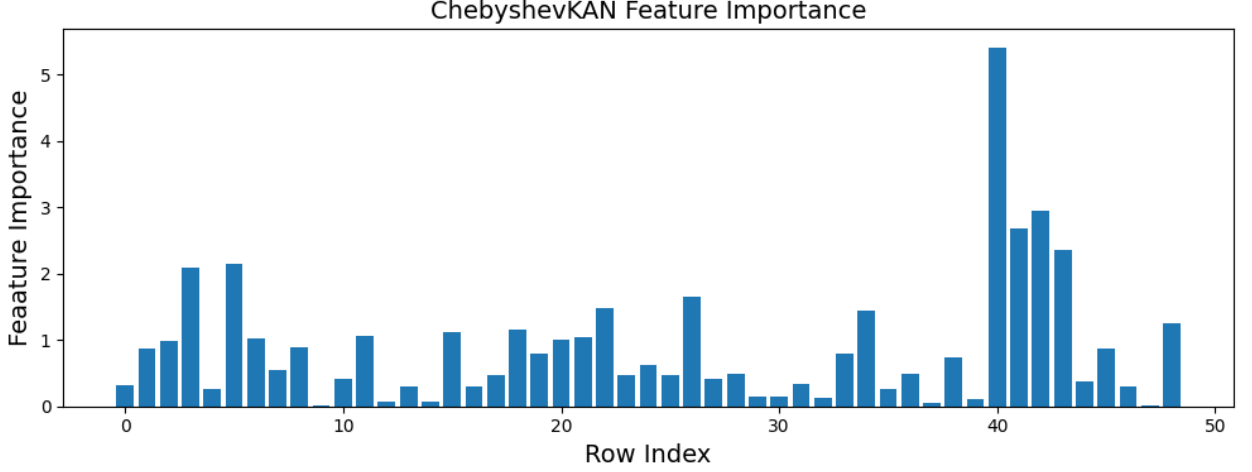


Fig. 7: Feature Importance based on ChebyshevKAN

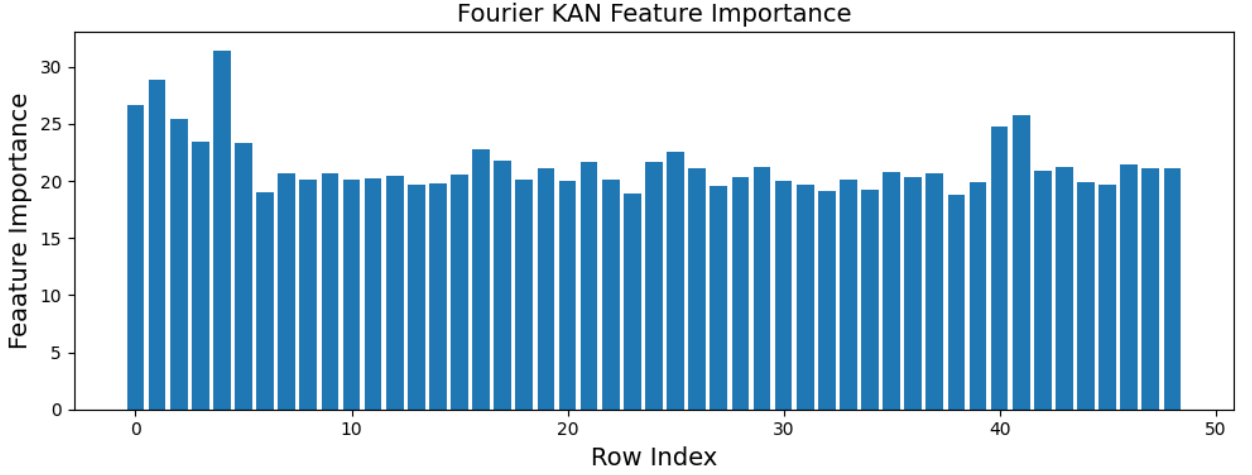


Fig. 8: Feature Importance based on Fourier KAN

we compute the absolute values of the coefficients from the Chebyshev equation in 1 and the Fourier equation in 2. Figure 7 depicts the ranked feature importance derived from the Chebyshev coefficients, while Figure 8 illustrates the corresponding rankings from the Fourier coefficients.

Based on these rankings, we conducted further experiments to assess the predictive performance of Fourier KAN and Chebyshev KAN models using subsets of features identified by their coefficients. Figures 9 and 10 illustrate the ROC-AUC performance across five datasets (CG, CA, DS, CB, BL) after varying levels of feature reduction. The results indicate that utilizing all available features does not necessarily yield the best predictive performance. In fact, for some datasets, models trained on reduced feature sets achieve comparable or even superior accuracy. This highlights TabKAN’s effectiveness in selecting compact, informative subsets of features, providing a valuable mechanism for supervised dimensionality reduction. Such an approach simplifies model interpretation and often enhances predictive robustness, further demonstrating the practical utility of the proposed TabKAN architectures.

Figure 11a reports the AUC values obtained using various subsets of top-ranked features identified by the proposed FourierKAN-based method, compared with those selected by SHAP analysis. The results demonstrate that model-specific feature importance consistently yields superior AUC performance when less significant features are removed.

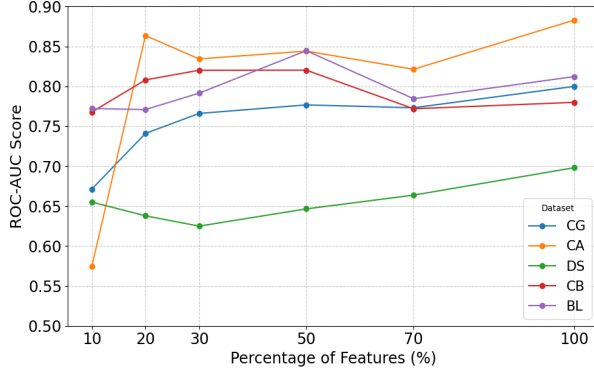


Fig. 9: AUC vs Percentage of Top Selected Features for Fourier KAN

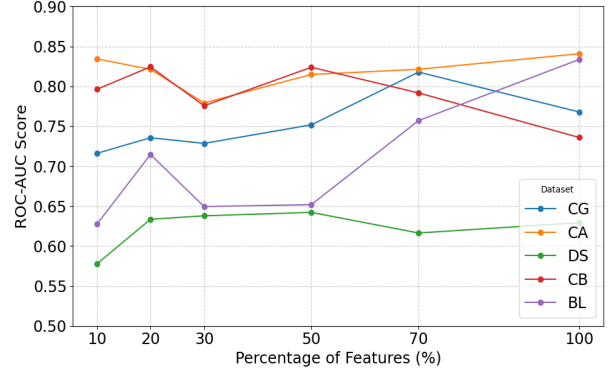


Fig. 10: AUC vs Percentage of Top Selected Features for ChebyshevKAN

Similarly, experiments conducted with ChebyshevKAN using the CG and CB datasets (Figure 11b) reinforce the observation that the proposed approach outperforms SHAP-based feature selection in achieving stable and improved predictive accuracy. While there is some overlap in the selected features between the SHAP-based and model-specific methods, the proposed approach often provides more stable or higher predictive performance. This outcome highlights the advantage of using learned functional parameters as a built-in mechanism for feature selection, which is both efficient and closely aligned with the model’s internal representation.

5 Ablation Study

5.1 Fine-tuning

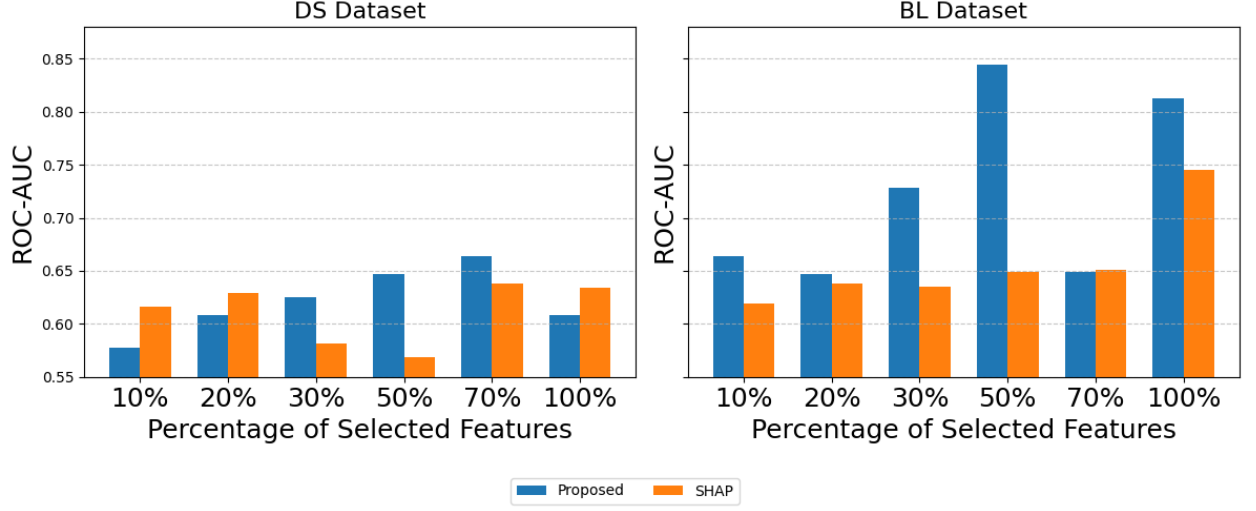
In transfer learning scenarios, where a pre-trained model is adapted to a new task or domain, the **Group Relative Policy Optimization (GRPO)** [44] framework provides a robust mechanism for fine-tuning by balancing task-specific adaptation and knowledge retention. Using a policy gradient method, GRPO optimizes model parameters θ through advantage-weighted updates derived from reward signals ($R \in \{0, 1\}$), which measure the alignment between sampled predictions ($o \sim \pi_\theta$) and ground-truth labels. To address catastrophic forgetting—a typical issue in transfer learning—the method includes a Kullback-Leibler (KL) divergence penalty $\beta \cdot \mathbb{D}_{\text{KL}}(\pi_\theta \parallel \pi_{\text{ref}})$, which constrains deviations from the reference policy π_{ref} (e.g., the original pre-trained model). By sampling G candidate predictions per input and calculating normalized advantages $\hat{A} = R - \mathbb{E}[R]$, GRPO promotes exploration while maintaining stability, making it well-suited for tasks with limited target-domain data.

$$\mathcal{J}_{\text{GRPO}}(\theta) = \underbrace{\mathbb{E}_{q \sim \text{Batch}} \left[\frac{1}{G} \sum_{i=1}^G \log \pi_\theta(o_i | q) \cdot \hat{A}_i \right]}_{\text{Policy Gradient Loss}} + \underbrace{\beta \cdot \mathbb{E}_{q \sim \text{Batch}} [\mathbb{D}_{\text{KL}}(\pi_\theta(\cdot | q) \parallel \pi_{\text{ref}}(\cdot | q))]}_{\text{KL Divergence Penalty}}$$

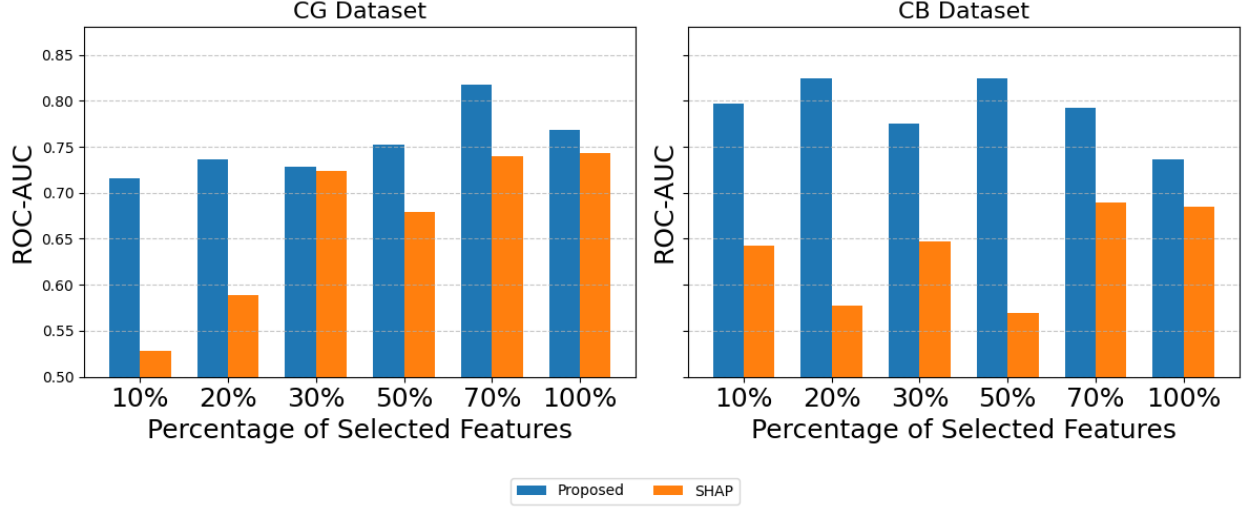
$$\hat{A}_i = R_i - \mathbb{E}[R_i] \quad (\text{Advantage})$$

$$R_i = \begin{cases} 1 & \text{if prediction } o_i = \text{label} \\ 0 & \text{otherwise} \end{cases}$$

$$\mathbb{D}_{\text{KL}}(\pi_\theta \parallel \pi_{\text{ref}}) = \sum_{c \in \{0,1\}} \pi_\theta(c | q) \log \frac{\pi_\theta(c | q)}{\pi_{\text{ref}}(c | q)}$$



(a) Comparison of Selective top important features in FourierKAN



(b) Comparison of Selective top important features in ChebyshevKAN

Fig. 11: Comparison of feature importance selection between the proposed method and SHAP across two datasets.

$$\mathcal{J}_{\text{GRPO}}(\theta) = -\mathbb{E} [\log \pi_{\theta}(o|q) \cdot \hat{A}] + \beta \cdot \mathbb{E} [\mathbb{D}_{\text{KL}}(\pi_{\theta} \parallel \pi_{\text{ref}})]$$

5.2 Ablation on Enhanced Architecture

We conducted an ablation study to develop a KAN-based architecture. As KAN serves as an alternative to MLP, we applied it to the MLP-Mixer [45] block to construct a KAN-Mixer [46]. Specifically, we replaced all MLP blocks in [25] (Fig. 2) with alternative KAN layers, preserving the overall structure of the original architecture while leveraging the functional properties of KAN. The results show improvements on certain datasets compared to the KAN-based models in Table 5, with these improvements marked by an asterisk. This indicates that the KAN-Mixer outperforms both

standard MLP-Mixer and basic KAN-based models on specific datasets, demonstrating its effectiveness in capturing complex patterns in tabular data. For reference, the results of the MLP-Mixer are taken from Table 2 in [25].

Table 5: Evaluation of Different Enhanced Models for Supervised Learning

Methods	CG	CA	DS	CB	BL	IO
ChebyshevKAN-Mixer	0.824*	0.863	0.706*	0.807	0.832	0.950
JacobiKAN-Mixer	0.817	0.876*	0.715*	0.767	0.843*	0.950
Fourier KAN-Mixer	0.850*	0.909*	0.715*	0.826*	0.707*	0.914

6 Conclusion

In this work, we introduced TabKAN, a novel Kolmogorov-Arnold Network-based architecture designed to advance tabular data analysis. By leveraging modular KAN-based models, we demonstrated their effectiveness in both supervised learning and transfer learning, where TabKAN significantly outperformed classical and Transformer-based models in knowledge transfer tasks. Unlike conventional deep learning approaches that rely on post hoc interpretability methods, TabKAN introduces model-specific interpretability, allowing for direct visualization and analysis of feature interactions within the network. To further enhance the expressiveness and adaptability of KANs for tabular data learning, we utilized multiple specialized architectures, including ChebyshevKAN, JacobiKAN, PadeRKAN, FourierKAN, fKAN, and fast-KAN, each offering distinct advantages in function approximation and performance. Additionally, we introduced a new fine-tuning approach for transfer learning, improving the efficiency of knowledge transfer between domains. Furthermore, we enhanced the basic architecture by leveraging the advantages of KAN over MLP, leading to the development of more robust and scalable models for tabular data. Our experiments across multiple benchmark datasets highlight the robustness, efficiency, and scalability of KAN-based architectures, bridging the gap between traditional machine learning and deep learning for structured data. Building on these advancements, future work will focus on further optimizing KAN architectures and extending their applicability to self-supervised learning and domain adaptation, enabling broader adoption of KANs in real-world applications.

7 Acknowledgements

We thank the creators of the public datasets and the authors of the baseline models for making these resources available for research. We gratefully acknowledge Brian Gold, PhD, and the Gold Lab at the University of Kentucky for their support and for providing the facilities necessary to carry out this research. This research is supported in part by the NSF under Grant IIS 2327113 and the NIH under Grants R21AG070909, P30AG072946, and R01HD101508-01.

References

- [1] Liu, Z., Wang, Y., Vaidya, S., Ruehle, F., Halverson, J., Soljačić, M., Hou, T.Y., Tegmark, M.: Kan: Kolmogorov-arnold networks. arXiv preprint arXiv:2404.19756 (2024)
- [2] SS, S., AR, K., KP, A., et al.: Chebyshev polynomial-based kolmogorov-arnold networks: An efficient architecture for nonlinear function approximation. arXiv preprint arXiv:2405.07200 (2024)
- [3] Aghaei, A.A.: rkan: Rational kolmogorov-arnold networks. arXiv preprint arXiv:2406.14495 (2024)
- [4] Dong, Y., Li, G., Tao, Y., Jiang, X., Zhang, K., Li, J., Su, J., Zhang, J., Xu, J.: Fan: Fourier analysis networks. arXiv preprint arXiv:2410.02675 (2024)
- [5] Aghaei, A.A.: fkan: Fractional kolmogorov-arnold networks with trainable jacobi basis functions. arXiv preprint arXiv:2406.07456 (2024)

- [6] Li, Z.: Kolmogorov-arnold networks are radial basis function networks. arXiv preprint arXiv:2405.06721 (2024)
- [7] Thapa, A., Kang, J., Chung, M.L., Wu, J.-R., Biddle, M.J., Cha, G., Moser, D.K.: Self-care, perceived social support, and health-related quality of life in persons with heart failure. *Nursing Research*, 10–1097 (2022)
- [8] Maqbool, M.H., Fereidouni, M., Siddique, A., Foroosh, H.: Model-agnostic zero-shot intent detection via contrastive transfer learning. *International Journal of Semantic Computing* **18**(1) (2024)
- [9] Ye, A., Wang, Z.: *Modern deep learning for tabular data: novel approaches to common modeling problems*. Springer (2023)
- [10] Chen, T., Guestrin, C.: Xgboost: A scalable tree boosting system. *Proceedings of ACM SIGKDD International Conference on Knowledge Discovery and Data Mining* **22**, 785–794 (2016)
- [11] Zhang, Y., Tong, J., Wang, Z., Gao, F.: Customer transaction fraud detection using xgboost model. *International Conference on Computer Engineering and Application (ICCEA)*, 554–558 (2020). IEEE
- [12] Klambauer, G., Unterthiner, T., Mayr, A., Hochreiter, S.: Self-normalizing neural networks. *Advances in Neural Information Processing Systems* **30**, 972–981 (2017)
- [13] Song, W., Shi, C., Xiao, Z., Duan, Z., Xu, Y., Zhang, M., Tang, J.: AutoInt: Automatic feature interaction learning via self-attentive neural networks. *ACM International Conference on Information and Knowledge Management*, 1161–1170 (2019)
- [14] Wang, Z., Sun, J.: Transtab: Learning transferable tabular transformers across tables. *Advances in Neural Information Processing Systems* **35**, 2902–2915 (2022)
- [15] Huang, X., Khetan, A., Cvitkovic, M., Karnin, Z.: Tabtransformer: Tabular data modeling using contextual embeddings. arXiv preprint arXiv:2012.06678 (2020)
- [16] Somepalli, G., Goldblum, M., Schwarzschild, A., Bruss, C.B., Goldstein, T.: Saint: Improved neural networks for tabular data via row attention and contrastive pre-training. arXiv preprint arXiv:2106.01342 (2021)
- [17] Dorogush, A.V., Ershov, V., Gulin, A.: Catboost: gradient boosting with categorical features support. arXiv preprint arXiv:1810.11363 (2018)
- [18] Ke, G., Meng, Q., Finley, T., Wang, T., Chen, W., Ma, W., Ye, Q., Liu, T.-Y.: Lightgbm: A highly efficient gradient boosting decision tree. *Advances in Neural Information Processing Systems* **30** (2017)
- [19] Onishi, S., Oono, K., Hayashi, K.: Tabret: Pre-training transformer-based tabular models for unseen columns. arXiv preprint arXiv:2303.15747 (2023)
- [20] Zhu, B., Shi, X., Erickson, N., Li, M., Karypis, G., Shoaran, M.: Xtab: Cross-table pretraining for tabular transformers. arXiv preprint arXiv:2305.06090 (2023)
- [21] Zarlenga, M.E., Shams, Z., Nelson, M.E., Kim, B., Jamnik, M.: Tabcbm: Concept-based interpretable neural networks for tabular data. *Transactions on Machine Learning Research* (2023)
- [22] Hollmann, N., Müller, S., Purucker, L., Krishnakumar, A., Körfer, M., Hoo, S.B., Schirrmeister, R.T., Hutter, F.: Accurate predictions on small data with a tabular foundation model. *Nature* **637**(8045), 319–326 (2025)
- [23] Yan, R., Islam, M.T., Xing, L.: Interpretable discovery of patterns in tabular data via spatially semantic topographic maps. *Nature Biomedical Engineering*, 1–12 (2024)

- [24] Li, J., Qian, R., Tan, Y., Li, Z., Chen, L., Liu, S., Wu, J., Chai, H.: Tabsal: Synthesizing tabular data with small agent assisted language models. *Knowledge-Based Systems* **304**, 112438 (2024)
- [25] Eslamian, A., Cheng, Q.: Tabmixer: advancing tabular data analysis with an enhanced mlp-mixer approach. *Pattern Analysis and Applications* **28**(2), 1–17 (2025)
- [26] Liu, Z., Wang, Y., Vaidya, S., Ruehle, F., Halverson, J., Soljačić, M., Hou, T.Y., Tegmark, M.: Kan: Kolmogorov-arnold networks. *arXiv preprint arXiv:2404.19756* (2024)
- [27] Ba, J.L., Kiros, J.R., Hinton, G.E.: Layer normalization. *arXiv preprint arXiv:1607.06450* (2016)
- [28] Xu, J., Chen, Z., Li, J., Yang, S., Wang, W., Hu, X., Ngai, E.C.-H.: Fourierkan-gcf: Fourier kolmogorov-arnold network—an effective and efficient feature transformation for graph collaborative filtering. *arXiv preprint arXiv:2406.01034* (2024)
- [29] Aghaei, A.A.: fkan: Fractional kolmogorov–arnold networks with trainable jacobi basis functions. *Neurocomputing* **623**, 129414 (2025)
- [30] Aghaei, A.A.: rkan: Rational kolmogorov-arnold networks. *arXiv preprint arXiv:2406.14495* (2024)
- [31] Akiba, T., Sano, S., Yanase, T., Ohta, T., Koyama, M.: Optuna: A next-generation hyperparameter optimization framework. In: *Proceedings of the 25th ACM SIGKDD International Conference on Knowledge Discovery & Data Mining*, pp. 2623–2631 (2019)
- [32] Kermani, A., Zeraatkar, E., Irani, H.: Energy-efficient transformer inference: Optimization strategies for time series classification. *arXiv preprint arXiv:2502.16627* (2025)
- [33] Arik, S.Ö., Pfister, T.: Tabnet: Attentive interpretable tabular learning. In: *Proceedings of the AAAI Conference on Artificial Intelligence*, vol. 35, pp. 6679–6687 (2021)
- [34] Wang, R., Fu, B., Fu, G., Wang, M.: Deep & cross network for ad click predictions. *Proceedings of the ADKDD’17* (2017) <https://doi.org/10.1145/3124749.3124754>
- [35] Gorishniy, Y., Rubachev, I., Khrulkov, V., Babenko, A.: Revisiting deep learning models for tabular data. *Advances in Neural Information Processing Systems* **34**, 18932–18943 (2021)
- [36] Yoon, J., Zhang, Y., Jordon, J., Schaar, M.: Vime: Extending the success of self-and semi-supervised learning to tabular domain. *Advances in Neural Information Processing Systems* **33**, 11033–11043 (2020)
- [37] Bahri, D., Jiang, H., Tay, Y., Metzler, D.: Scarf: Self-supervised contrastive learning using random feature corruption. *arXiv preprint arXiv:2106.15147* (2021)
- [38] Bozorgasl, Z., Chen, H.: Wav-kan: Wavelet kolmogorov-arnold networks. *arXiv preprint arXiv:2405.12832* (2024)
- [39] Ta, H.-T., Thai, D.-Q., Rahman, A.B.S., Sidorov, G., Gelbukh, A.: Fc-kan: Function combinations in kolmogorov-arnold networks. *arXiv preprint arXiv:2409.01763* (2024)
- [40] Deldadehasl, M., Karahroodi, H.H., Nekah, P.H.: Customer clustering and marketing optimization in hospitality: A hybrid data mining and decision-making approach from an emerging economy (2025)
- [41] Su, A., Wang, A., Ye, C., Zhou, C., Zhang, G., Chen, G., Zhu, G., Wang, H., Xu, H., Chen, H., et al.: Tablegpt2: A large multimodal model with tabular data integration. *arXiv preprint arXiv:2411.02059* (2024)

- [42] Huang, W.: Multimodal contrastive learning and tabular attention for automated alzheimer’s disease prediction. In: Proceedings of the IEEE/CVF International Conference on Computer Vision, pp. 2473–2482 (2023)
- [43] Gao, W., Gong, Z., Deng, Z., Rong, F., Chen, C., Ma, L.: Tabkanet: Tabular data modeling with kolmogorov-arnold network and transformer. arXiv preprint arXiv:2409.08806 (2024)
- [44] Shao, Z., Wang, P., Zhu, Q., Xu, R., Song, J., Bi, X., Zhang, H., Zhang, M., Li, Y., Wu, Y., et al.: Deepseekmath: Pushing the limits of mathematical reasoning in open language models. arXiv preprint arXiv:2402.03300 (2024)
- [45] Tolstikhin, I.O., Houlsby, N., Kolesnikov, A., Beyer, L., Zhai, X., Unterthiner, T., Yung, J., Steiner, A., Keysers, D., Uszkoreit, J., *et al.*: Mlp-mixer: An all-mlp architecture for vision. Advances in neural information processing systems **34**, 24261–24272 (2021)
- [46] Ibrahim, A.D.M., Shang, Z., Hong, J.-E.: How resilient are kolmogorov–arnold networks in classification tasks? a robustness investigation. Applied Sciences **14**(22), 10173 (2024)

Appendix A Hyperparameter Sensitivity

This appendix provides a detailed analysis of the hyperparameter sensitivity across seven neural network models (fastKAN, RKAN, fKAN, ChebKAN, KAN, FourierKAN) evaluated on eight datasets (IO, IC, DS, CG, CB, CA, BL, AD). The analysis focuses on four key architectural metrics: Layers, Neurons, Order, and Grid, as summarized in Tables [A1](#), [A2](#), [A3](#), [A4](#), [A5](#), [A6](#), [A7](#), and [A8](#).

The architectural complexity of the models varies significantly, with distinct patterns emerging in terms of depth, width, and approximation strategies. The RKAN and fKAN models consistently employ the highest number of layers, with RKAN reaching up to 7.7 layers in the BL dataset and fKAN averaging 7.5 layers in the IC and CA datasets. This suggests a reliance on depth to capture complex patterns. In contrast, fastKAN and ChebKAN use fewer layers, typically ranging from 1.5 to 3.5 on average, favoring simpler architectures. The variability in the number of layers is particularly high for RKAN and ChebKAN, as indicated by their large standard deviations (e.g., ChebKAN: std=2.6 in DS), reflecting dataset-specific adjustments in depth.

In terms of width, ChebKAN consistently uses the most neurons, with means ranging from 114 to 134 across datasets, followed by fastKAN, which averages between 105 and 149 neurons. This indicates a preference for wide, high-capacity layers. On the other hand, KAN and FourierKAN are the most compact, with KAN averaging 11.7 to 41.1 neurons and FourierKAN averaging 33.1 to 46.9 neurons. The stability of neuron counts also varies across models. KAN exhibits low variability (std=3.8–8.4), suggesting consistent architectural choices, while ChebKAN and fastKAN show high variability (e.g., ChebKAN: std=57.9 in BL), indicating dataset-specific tuning.

The order of basis functions, which reflects the complexity of the approximation, also varies across models. ChebKAN and fKAN use the highest-order basis functions, with ChebKAN averaging 4.2 to 5.4 and fKAN averaging 3.0 to 4.1. This likely enables precise approximations but may increase computational cost. In contrast, KAN uses the lowest order, averaging 1.1 to 2.9, favoring simpler models. Notably, fastKAN and FourierKAN do not use order parameters, implying fixed or non-polynomial basis functions.

Grid-based approximations are employed by KAN and FourierKAN, with FourierKAN utilizing the largest grids, averaging 10.2 in the BL dataset. This suggests the use of grid-based methods, such as Fourier transforms or splines, to achieve adaptive resolution. The variability in grid sizes is significant, particularly for FourierKAN (std=2.6 in BL), indicating adjustments based on dataset complexity.

Dataset-specific trends further highlight the adaptability of these models. For example, in the IO dataset, ChebKAN uses the widest layers (mean=121 neurons), while KAN is the most efficient (mean=41.1 neurons). In the IC dataset, KAN has the smallest architecture (mean=13.7 neurons), contrasting with fastKAN (mean=149.3 neurons). The AD dataset showcases ChebKAN using the highest order (mean=5.4), while fastKAN has the lowest neuron count (mean=46.4) but higher depth (mean=3.5 layers). In the BL dataset, RKAN and fKAN are the deepest (mean=7.7 and 6.4 layers, respectively), while FourierKAN uses the largest grid (mean=10.2).

The trade-offs between depth, width, and approximation strategies are evident. Models like RKAN and fKAN prioritize depth, while ChebKAN and fastKAN emphasize width. KAN strikes a balance, maintaining compact architectures. The choice of approximation strategy also varies, with ChebKAN and fKAN relying on high-order polynomials for accuracy, and KAN and FourierKAN using grid-based methods. Low-variability models, such as KAN, offer consistency, while high-variability models, such as ChebKAN, adapt to dataset complexity.

For practitioners, these insights provide guidance on model selection. ChebKAN or fastKAN are suitable for high-dimensional data due to their wide layers and high capacity. KAN and FourierKAN are ideal for efficiency, given their compact architectures and grid-based approximations. For tasks requiring the capture of complex patterns, RKAN and fKAN leverage depth and high-order approximations effectively.

Model	Layers		Neurons		Order		Grid	
	Mean	Std.	Mean	Std.	Mean	Std.	Mean	Std.
fastKAN	1.3	0.5	144.5	39.2	-	-	-	-
JacobiRKAN	1.5	0.8	77.0	13.0	2.2	0.4	-	-
PadéRKAN	2.8	1.4	124.7	30.1	(5.0, 2.3)	(0.6, 0)	-	-
fKAN	4.9	1.1	71.1	11.1	3.9	0.6	-	-
ChebKAN	2.1	0.3	123.2	25.1	4.9	0.3	-	-
KAN	1.0	0.0	40.0	0.0	1.0	0.0	7.0	0.0
FourierKAN	2.6	0.6	37.2	6.3	-	-	1.9	0.6

Table A1: IO Dataset

Model	Layers		Neurons		Order		Grid	
	Mean	Std.	Mean	Std.	Mean	Std.	Mean	Std.
fastKAN	2.4	0.7	156.2	20.5	-	-	-	-
JacobiRKAN	1.9	1.5	19.0	10.0	3.7	0.6	-	-
PadéRKAN	4.0	1.2	98.0	39.6	(4.5, 2.9)	(0.5, 1)	-	-
fKAN	7.6	1.8	43.3	7.9	3.9	0.4	-	-
ChebKAN	1.0	0.0	141.4	36.4	5.1	0.6	-	-
KAN	2.0	0.0	10.0	0.0	1.0	0.0	5.0	0.0
FourierKAN	1.0	0.2	52.9	10.1	-	-	4.5	3.0

Table A2: IC Dataset

Model	Layers		Neurons		Order		Grid	
	Mean	Std.	Mean	Std.	Mean	Std.	Mean	Std.
fastKAN	1.4	0.7	105.8	35.9	-	-	-	-
JacobiRKAN	4.6	2.3	59.1	11.1	3.2	0.7	-	-
PadéRKAN	10.7	7.0	92.5	29.3	(3.9, 3.7)	(0.3, 1)	-	-
fKAN	7.4	1.8	58.6	7.6	4.0	0.4	-	-
ChebKAN	2.1	0.6	125.1	40.2	4.6	0.7	-	-
KAN	3.6	0.5	20.4	2.8	3.0	0.0	3.0	0.0
FourierKAN	2.1	0.4	39.4	8.1	-	-	6.6	1.5

Table A3: DS Dataset

Model	Layers		Neurons		Order		Grid	
	Mean	Std.	Mean	Std.	Mean	Std.	Mean	Std.
fastKAN	1.7	0.8	116.0	27.6	-	-	-	-
JacobiRKAN	1.4	0.8	86.9	13.6	2.4	0.6	-	-
PadéRKAN	3.0	1.3	126.7	27.6	(4.8, 3.2)	(0.7, 0)	-	-
fKAN	3.3	1.9	70.7	12.9	2.9	0.5	-	-
ChebKAN	2.6	0.5	116.0	20.4	4.3	0.7	-	-
KAN	3.0	0.0	26.7	0.0	3.0	0.0	5.0	0.0
FourierKAN	2.4	0.7	38.4	9.3	-	-	2.1	1.0

Table A4: CG Dataset

Model	Layers		Neurons		Order		Grid	
	Mean	Std.	Mean	Std.	Mean	Std.	Mean	Std.
fastKAN	1.3	0.6	113.7	34.7	-	-	-	-
JacobiRKAN	2.8	2.1	70.2	16.3	3.0	0.3	-	-
PadéRKAN	15.2	5.7	105.7	8.9	(4.0, 4.3)	(0.2, 0)	-	-
fKAN	3.4	1.0	44.4	11.0	3.2	0.6	-	-
ChebKAN	2.5	0.5	122.1	30.9	4.4	0.5	-	-
KAN	3.0	0.0	10.0	0.0	1.0	0.0	5.0	0.0
FourierKAN	2.3	0.5	34.7	11.9	-	-	2.6	0.8

Table A5: CB Dataset

Model	Layers		Neurons		Order		Grid	
	Mean	Std.	Mean	Std.	Mean	Std.	Mean	Std.
fastKAN	2.8	0.7	126.9	23.6	-	-	-	-
JacobiRKAN	1.2	0.8	64.3	23.5	2.2	0.6	-	-
PadéRKAN	3.4	2.0	99.9	24.0	(5.0, 3.6)	(0.6, 1)	-	-
fKAN	7.4	1.5	56.9	8.3	3.9	0.4	-	-
ChebKAN	2.0	0.8	118.4	31.0	2.3	0.5	-	-
KAN	6.7	0.5	26.0	1.6	1.0	0.1	1.0	0.2
FourierKAN	2.3	0.5	32.4	7.1	-	-	4.8	1.3

Table A6: CA Dataset

Appendix B Dataset links

We provide the links for the public datasets that we used for the benchmark. Details of each dataset can be found in Table B9.

Model	Layers		Neurons		Order		Grid	
	Mean	Std.	Mean	Std.	Mean	Std.	Mean	Std.
fastKAN	2.5	0.7	113.8	23.5	-	-	-	-
JacobiRKAN	8.0	1.5	70.3	7.3	3.5	0.4	-	-
PadéRKAN	2.3	1.6	137.3	32.2	(4.4, 2.4)	(0.7, 1)	-	-
fKAN	6.4	0.9	66.2	8.3	3.6	0.4	-	-
ChebKAN	1.1	0.3	130.3	64.5	4.0	1.4	-	-
KAN	2.0	0.2	35.4	3.3	1.0	0.1	6.1	1.1
FourierKAN	1.0	0.1	35.1	9.7	-	-	11.0	2.3

Table A7: BL Dataset

Model	Layers		Neurons		Order		Grid	
	Mean	Std.	Mean	Std.	Mean	Std.	Mean	Std.
fastKAN	3.6	1.8	35.8	22.1	-	-	-	-
JacobiRKAN	3.5	1.2	24.2	10.9	2.9	0.4	-	-
PadéRKAN	2.7	1.4	121.1	26.9	(3.8, 4.4)	(0.8, 1)	-	-
fKAN	5.4	1.8	33.0	7.3	3.3	0.8	-	-
ChebKAN	1.0	0.2	44.9	26.5	5.7	0.8	-	-
KAN	4.3	0.7	24.3	1.8	2.0	0.0	3.0	0.0
FourierKAN	1.0	0.2	44.9	8.1	-	-	8.8	2.7

Table A8: AD Dataset

Table B9: Benchmark Dataset Links

Dataset	URL
Credit-G	https://www.openml.org/search?type=data&status=active&id=31
Credit-Approval	https://archive.ics.uci.edu/ml/datasets/credit+approval
Dress-Sales	https://www.openml.org/search?type=data&status=active&id=23381
Adult	https://www.openml.org/search?type=data&status=active&id=1590
Cylinder-Bands	https://www.openml.org/search?type=data&status=active&id=6332
Blastchar	https://www.kaggle.com/datasets/blatchar/telco-customer-churn
Insurance-Co	https://archive.ics.uci.edu/ml/datasets/Insurance+Company+Benchmark+(COIL+2000)
1995-Income	https://www.kaggle.com/datasets/lodetomasi1995/income-classification
ImageSegmentation	https://www.openml.org/search?type=data&sort=version&status=any&order=asc&exact_name=segment&id=36
ForestCovertime	https://archive.ics.uci.edu/dataset/31/covertime

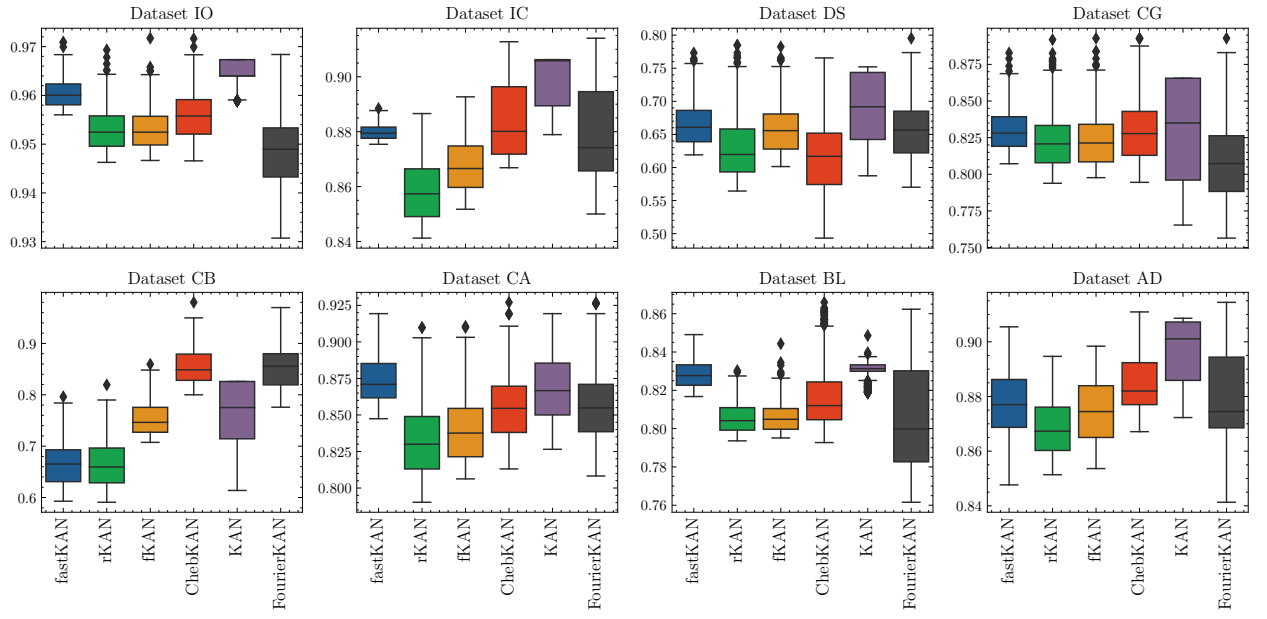


Fig. A1: The interquartile range across 100 runs with varying hyperparameters highlights the influence of architecture on experimental outcomes. The plot depicts the variation in the distribution of raw and synthesized data across different training and test set splits.